United States
Department of
Agriculture

Forest Service

Southern
Research Station

Research Paper
SRS–44

A Discrete Global Grid for Photointerpretation

Joseph M. McCollum, Jamie K. Cochran, and Anita K. Rose

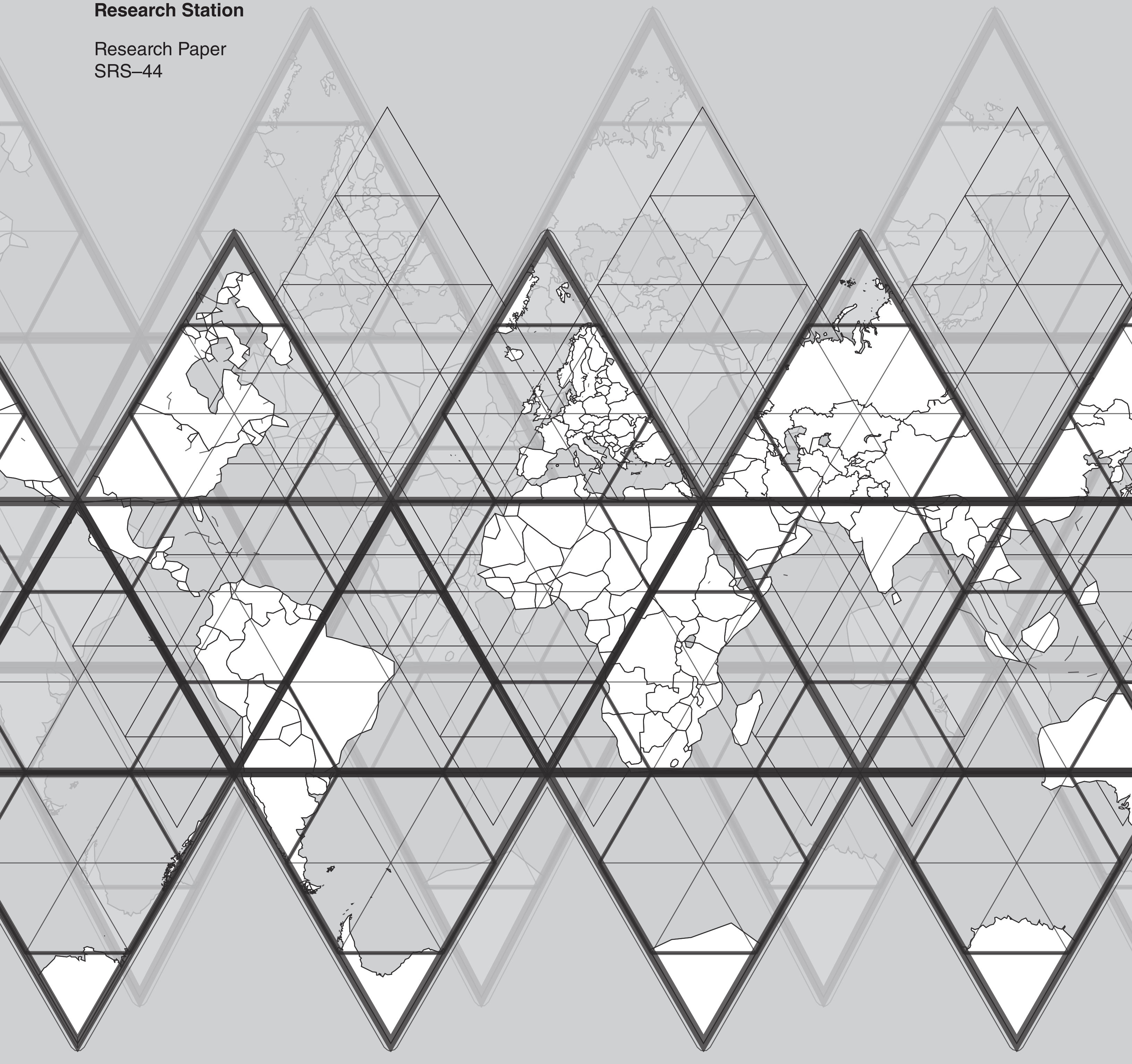

Authors:

Joseph M. McCollum, IT Specialist, **Jamie K. Cochran,** Supervisory Forester, and **Anita K. Rose,** Ecologist, Forest Inventory and Analysis Southern Research Station, Forest Service, U.S. Department of Agriculture, Knoxville, TN 37919.

July 2008

Southern Research Station
200 W.T. Weaver Blvd.
Asheville, NC 28804

A Discrete Global Grid for Photointerpretation

Joseph M. McCollum, Jamie K. Cochran, and Anita K. Rose

Abstract

The Forest Inventory and Analysis (FIA) Program of the Forest Service, U.S. Department of Agriculture, collects its data in three phases. The first phase is collection of photointerpretation data or dot counts, the second phase is field collection of FIA plot data, and the third phase is collection of Forest Health Monitoring data. This paper describes the development of the Phase 2 (P2) and Phase 3 (P3) grids and discusses the creation of a new grid for Phase 1 (P1), complete with an efficient indexing scheme, which is essentially equivalent to the historical dot count grids. The P2 grid consists of one field site per approximately 6,000 acres. To create the new P1 grid, we decomposed the P2 grid by a factor of 27 to obtain new proposed P1 photointerpretation cells of about 220 acres. The new grid can be used for initial photointerpretation points to determine area estimates forested land.

Keywords: FIA, Forest Health Monitoring, global grids, hexagon, Phase 1, Phase 2, Phase 3, photointerpretation.

Introduction

The Forest Inventory and Analysis (FIA) Program of the Forest Service, U.S. Department of Agriculture, is responsible for inventorying forested land in the United States and its possessions. A three-phase sampling procedure is used in conducting inventories. Within the Southern Research Station, forest area estimation Phase 1 (P1) has historically been accomplished by classifying aerial photographs on a forest/nonforest basis. In Phase 2 (P2), a subsample of P1 points is visited to confirm the classification and estimate tree and stand-level attributes. In Phase 3 (P3), a subset of the P2 plots is visited to evaluate forest health. The chief end product is a report of the forest conditions in each State (Conner and others 2004). The results are often reported by survey unit, an FIA-defined group of contiguous counties within a State that usually have similar ecological characteristics.

The hexagonal grid system FIA currently uses for sampling originated within the Environmental Protection Agency's Environmental Monitoring and Assessment Program (Overton and others 1990). It was adopted by the Forest Health Monitoring (FHM) Program but geometrically translated, and was subsequently adopted by FIA.

For P1 classification, photointerpreters have historically counted dots or clusters of dots on unrectified photos to obtain area estimates. Photointerpreters have called each dot forested land, nonforested land, census water, or noncensus water. Typically 25 dots or clusters of dots have been done per plot. This method has several weaknesses. At times, dots have not been across the entire landscape but have been concentrated near plots. Second, photointerpreters have written their results on paper; and these results have been transcribed by keypunching, so transcription errors have been possible. In addition, dots printed on the photograph could obscure the landscape and transparent overlays are not necessarily reproducible.

The objective of this study was to create an improved method for forest area estimation. The new method was to make use of a grid that conforms with the current P2 grid, with dot counts distributed evenly across the landscape, and was to be capable of being made operational quickly. The improved methodology we have developed includes a program to record the photointerpreters' call, to allow photointerpreters to see what is under the dot, and to allow a photointerpreter to check another's results.

Background

Figure 1 gives an idea of how global grids are developed. The base map data was obtained from the Global Resource Information Database of the United Nations Environment Programme (Global Resource Information Database-Geneva 1992) and projected onto an icosahedron via the gnomonic projection by the authors. Note that each face of the icosahedron has a different aspect.

An icosahedron is a solid having 20 faces that are shown in the figure as large equilateral triangles. Faces are outlined with wide white lines. Each triangle may be divided into nine smaller triangles, shown with thin black lines. Sets of six such triangles may be grouped to form a "mother hexagon" shown in medium black lines. This method also produces pentagons in 12 sets of 5 triangles.

Snyder (1992) showed how to project the earth onto any of the platonic solids, but specifically onto an icosahedron.

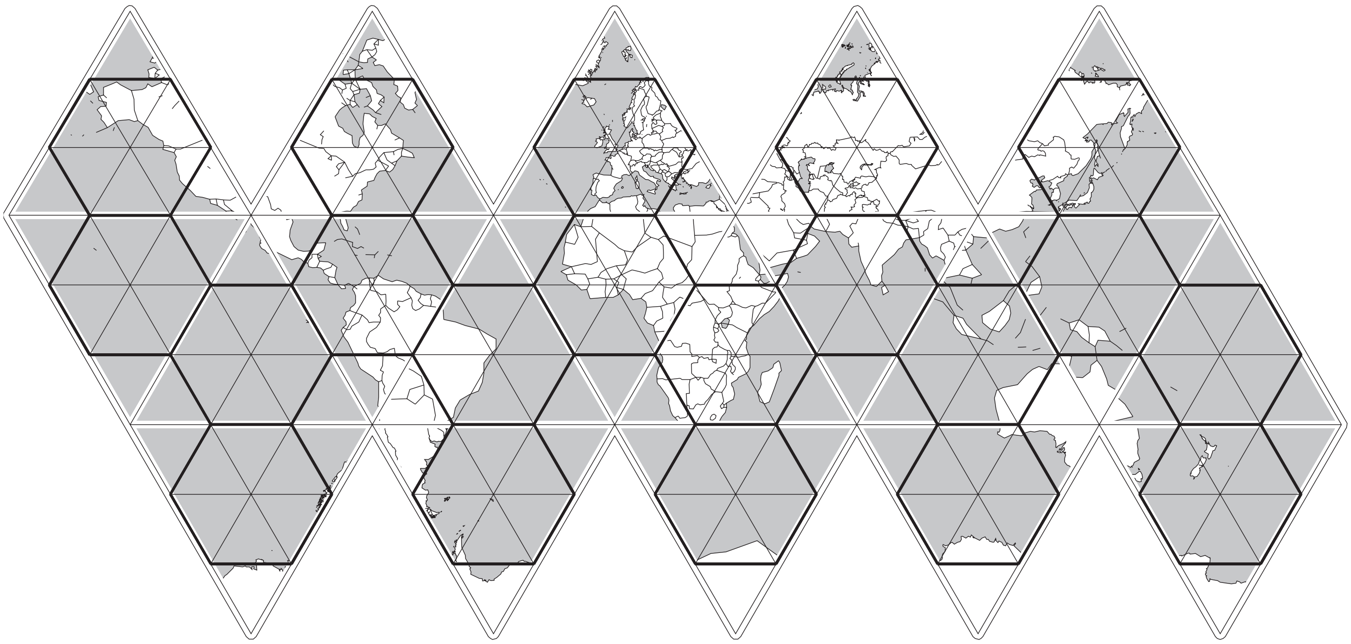

Figure 1—Earth projected on an icosahedron.

Today the projection is called the Icosahedral Snyder Equal Area (ISEA) projection (Carr and others 1997). It is not supported in widely used spatial software packages.

The surface area (adapted from Pearson 1990) of an ellipsoid is:

$$S = 4\pi R_A^2 = 4\pi a^2 \bullet (1 - e^2) \bullet \sum_{i=0}^{\infty} \tfrac{i+1}{2i+1} e^{2i} \qquad (1)$$

where

R_A = the authalic radius of the ellipsoid
a = the length of the semi-major axis of the ellipsoid
e = the eccentricity
i = an index variable

The authalic radius of an ellipsoid is the radius of a sphere with the same surface area as the given ellipsoid. Equation (1) leads us to an estimate of 5.10×10^{14} m^2 for the surface area of the earth, using either the Clarke 1866 ellipsoid (a = 6378206.4 m, e = 0.0823) or the Geodetic Reference System 1980 ellipsoid (a = 6378137 m, e = 0.0818), and consequently 1.70×10^{13} m^2 for the surface area of a mother hexagon. See ESRI (1991) for values of a and e for the Clarke 1866 and Geodetic Reference System 1980 ellipsoids.

Any hexagon may be decomposed into $T = h^2 + hk + k^2$ smaller hexagons, where h and k are any integers. Without loss of generality, it is possible to set $h \geq k \geq 0$ by reorienting axes. In virology, T is the "triangulation" number (Caspar and Klug 1962). Any product of triangulation numbers is also a triangulation number. In turn, the smaller hexagons may themselves be decomposed into smaller and smaller hexagons. The value for one iteration of T is the aperture, and the number of iterations of T is the resolution (Sahr and others 2003). A constant aperture size is preferred when defining the resolution, but mixed aperture sizes are possible in global grids. Common values of T include T = 3 (if h = 1, k = 1), which results in a hexagon consisting of one whole hexagon and six third-hexagons, as shown in figure 2A, and T = 4 (if h = 2, k = 0), which results in a hexagon consisting of one whole hexagon and six half-hexagons, as shown in figure 2B.

When the FIA and FHM grids were distributed to FIA units around the country, they were distributed as polygon and point coverages. When projected into the cone-based Albers Equal Area projection, the cell size is indeed 5,937.2 acres, with a range of < 1 acre (Brand and others 2000). When projected into the plane-based Lambert Azimuthal Equal Area (LAEA) projection, the cell size is about 5,931 acres, with a range of about 40 acres, depending on the choice of projection point. When projected into the cylinder-based Cylindrical Equal Area projection, the cell size is again

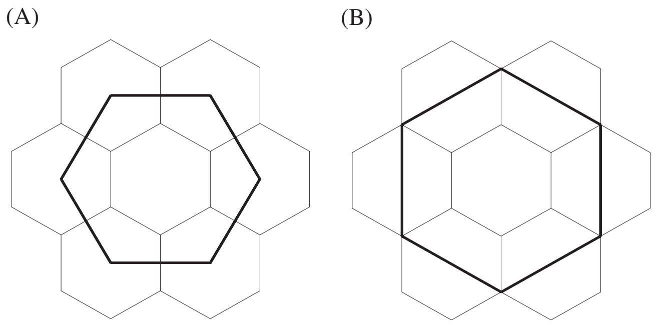

Figure 2—Simple decompositions of a hexagon.

about 5,931 acres, with a slightly smaller range of about 32 acres.

For sufficiently densified arcs, all equal area projections should yield the same result. For the P2 and P3 grids, hexagons are defined as sets of six points. The paths that connect one point to the next are implied. Thus, spatial software packages infer a straight line in the current projection. If paths from one point to the next were defined rigorously, each equal area projection would yield the same result, although shape would be distorted from one projection to the next.

Methods

Sahr and others (2003) list five design choices for constructing a global grid. The authors could not determine the design choices used in constructing the original FIA grid but desired a grid that would conform with it. First, the authors confirm that an icosahedron was used to construct the original grid. Second, the authors could not determine the orientation of the icosahedron. Third, they observe that if a mother hexagon is decomposed by a factor of 3, 11 times, and a factor of 4 once, the result is 2.40 x 108 m^2 (5,930 acres), the approximate size of a P2 hexagon. Fourth, they believe that the original projection method was ISEA, and since that was not available, that LAEA is the next best choice. Fifth, the authors have developed their own indexing system for the P2 grid (and consequently the P1 grid).

While use of the cone-based Albers projection results in lower variation in the size of a hexagon, the authors found that the plane-based LAEA projection preserves the shape of the hexagons better. Under the Albers projection, segment length and interior angles had a higher variation than they did under the LAEA projection. A cursory analysis of the FIA grids showed that the standard deviation of the interior angles of the Albers grid is about 1º; the standard deviation of the interior angles of the LAEA grid is about 0.1º. Moreover, White and others (1992) found that LAEA preserves geometry better than Albers.

Consequently, the authors started with the P2 grid and decomposed that one. Remember that cell sizes are not exactly equal under any supported projection, so it does not work to start with a hexagon of desired size and tessellate it over the plane. Beyond some distance, this grid would not conform with the P2 grid.

The authors thought about consistency with the past and considered a 25-fold decomposition (h = 5, k = 0), as shown in figure 3.

Constructing this decomposition requires not just collection of hexagon centers and vertices but also calculation of several intermediate points. Note that there is a point that is 3/5 the distance from the center to each of the vertices. Note also that for each segment of the hexagon, there are two additional points that are 2/5 and 4/5 the distance from the center to each of the segment midpoints. Note also that there are two points on each segment that are 1/5 and 4/5 the distance from one vertex to the next. Thus, there are a total of 19 points on the interior of the hexagon, and 12 other points are shared with one other hexagon (they count as one-half points), for a total of 25.

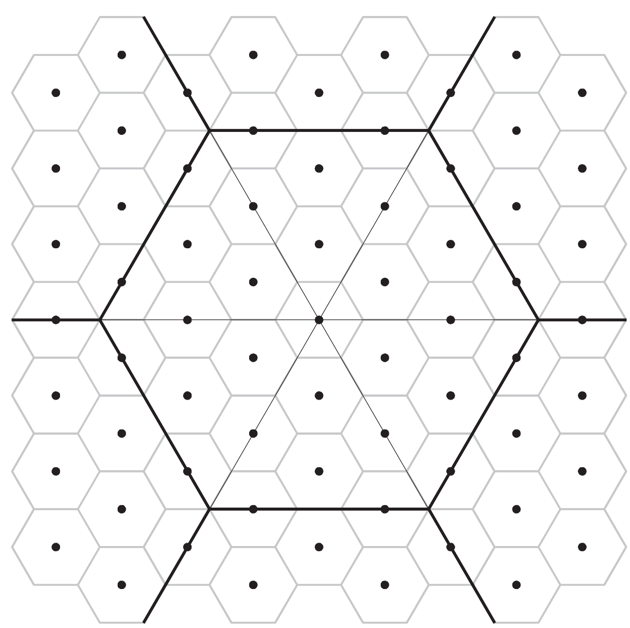

Figure 3—Twenty-five fold decomposition of a hexagon.

The only information that is required to construct a three-fold decomposition are the hexagon centers and the vertices, and performing a Thiessen expansion on those points. To simplify programming tasks, the authors opted for a 27-fold decomposition of the P1 grid.

Analysis of the grid is facilitated if cells are neatly numbered in rows and paths. Also, it is less work in the long run if the cells are numbered along the way rather than at the end of all iterations. Thus, a method of numbering the cells must be found.

The method actually used by the authors is the simple one described by White and others (1992). It is shown in figure 4. Ideally, one should start with the mother hexagon and number it as (0,0) for instance and derive new coordinates for each hexagon as it is created. Since this option was not available to the authors, they first painstakingly numbered the P2 cells in rows and paths. This process involved an iterative approach of guessing where centers would be, then finding which cells had no proposed center or more than one center. For the purposes of producing the P1 grid, the P2 grid is Resolution 1. The reader is also asked to imagine three sets of axes in figure 4. One set is the traditional east-west *x*-axis and the north-south *y*-axis. Another set is the r_1-axis, running from southwest to northeast, and the p_1-axis, which is coincident with the *y*-axis. The final set of axes

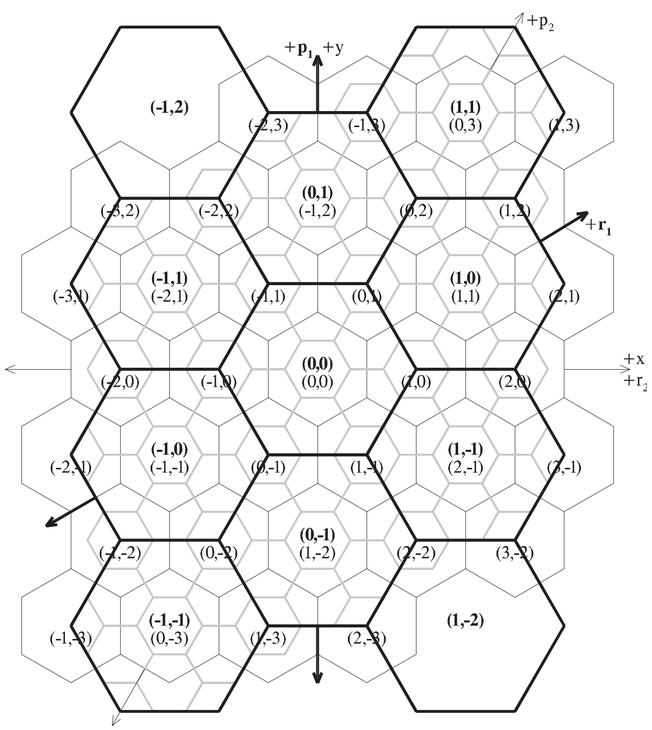

Figure 4—Resolution 1 (top coordinate) to Resolution 2 (bottom coordinate).

is the r_2-axis, coincident with the *x*-axis, and the p_2-axis, running from south-southwest to north-northeast.

If the cells of Resolution *i* are numbered in rows and paths as (r_i,p_i), then one way of relating Resolution 2 to Resolution 1 is to convert (r_i,p_i) to rectangular coordinates, as shown in equations (2) through (5).

$$x = \tfrac{3}{2} \bullet q \bullet r_1 \qquad (2)$$

$$y = \tfrac{\sqrt{3}}{2} \bullet q \bullet r_1 + \sqrt{3} \bullet q \bullet p_1 \qquad (3)$$

$$x = q \bullet r_2 + \tfrac{1}{2} \bullet q \bullet p_2 \qquad (4)$$

$$y = \tfrac{1}{2} \bullet \sqrt{3} \bullet q \bullet p_2 \qquad (5)$$

where

x = the *x*-coordinate (east) of a point
y = the *y*-coordinate (north) of a point
q = the circumscribed radius of a Resolution 1 hexagon
p_i = the path number of Resolution *i*
r_i = the row number of Resolution *i*

Set *x*'s and *y*'s in equations (2) through (5) equal to each other to get a system of two equations, which is solved for r_2 and p_2, yielding:

$$r_2 = r_1 - p_1 \qquad (6)$$

$$p_2 = r_1 + 2p_1 \qquad (7)$$

Thus, it is possible to calculate the row and path of a Resolution 2 hexagon from its parent Resolution 1 hexagon's row and path. The reader can verify that for cells sharing centers, such as the Resolution 1 (1,1) and the Resolution 2 (0,3), that indeed $r_2 = r_1 - p_1$ and $p_2 = r_1 + 2p_1$. An adjustment must be made for cells not sharing centers.

The program calculates the azimuth (starting from north) between the current point on the Resolution 2 grid and the corresponding Resolution 1 center. With this example, if the azimuth is near 30º, then add 1 to the path. If the azimuth is near 90º, then add 1 to the row. If the azimuth is near 150º, then add 1 to the row and subtract 1 from the path. If the azimuth is near 210º, subtract 1 from the path. If the azimuth is near 270º, then subtract 1 from the row. Finally, if the azimuth is near 330º, then subtract 1 from the row and add 1 to the path. In the program the authors have written for this exercise, they define "near" as ± 30º, although in reality, it is likely no more than a few degrees under the Albers projection and much less than that under the LAEA projection. However, the authors notice that the deviation can grow much larger near the edge of the grid; thus when processing a State or survey unit, the authors included a large buffer of about 0.5º of latitude and longitude around the area of interest.

Going from Resolution 2 to Resolution 3 is a little different. In figure 5, the Resolution 1 grid is shown in gray lines, the Resolution 2 grid is shown in thin black lines, and the Resolution 3 grid is shown in heavy lines and bold text.

In Resolution 3, the r_3-axis is coincident with the r_1-axis, and the p_3-axis is coincident with the p_1-axis. Rows of hexagons are vertical columns, and paths of hexagons go from southwest to northeast. A method similar to the one used for figure 4 shows the equations to be:

$$r_3 = 2r_2 + p_2 \tag{8}$$

$$p_3 = p_2 - r_2 \tag{9}$$

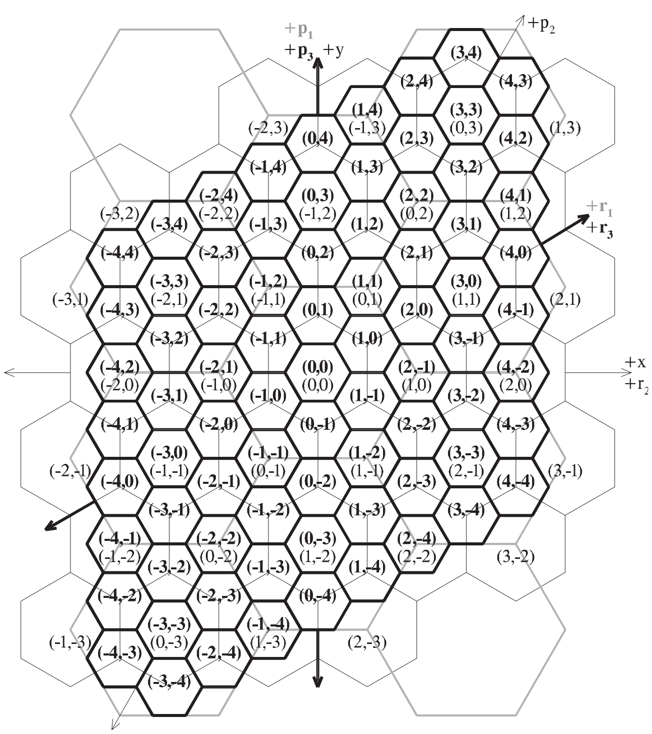

Figure 5—Resolution 2 (bottom coordinate) to Resolution 3 (top coordinate).

Again the reader can verify these equations hold true for the cells that share centers, e.g., that the Resolution 3 coordinates (0, -3) can be generated from the Resolution 2 coordinates (1, -2). The angular adjustments are 30º out of phase from the previous resolution—occurring at 0º, 60º, 120º, 180º, 240º, and 300º instead of 30º, 90º, 150º, 210º, 270º, and 330º.

Going from Resolution 3 to Resolution 4 is exactly like going from Resolution 1 to Resolution 2. At this point the authors stopped. However, some of FIA's partners have expressed interest in a more intense photointerpretation. This method could be easily adapted to higher resolutions of aperture 3. However, the authors do not see a way of generalizing the method to any arbitrary aperture size. Rather, a strategy would have to be developed for each aperture size. The authors have shown the strategy for T = 25, for example.

Results and Discussion

The authors have produced P1 grids for each of the Southern States. The grids are seamless along State lines and survey unit lines even for Texas, which was processed one survey unit at a time.

The authors' vision is that photointerpreters can use a digital orthophotograph or other digital image along with the grids the authors have created and a computer program to record the results.

In figure 6 we see an illustration of all three phases of FIA: the smallest cells, shown with fine black lines, are P1 photointerpretation cells. There are 27 P1 hexagons per P2 hexagon—19 whole hexagons plus 12 half-hexagons plus 6 third-hexagons. The medium-sized cells, shown in heavy dark gray lines, are P2 FIA cells. A cell of any phase belongs to the State where its center is. The large cells shown in heavy gray lines are P3 cells. P3 cells come in two types: one shown in figure 6A, called the C_{16}, consists of 13 whole P2 cells and one-half of 6 other P2 cells, for a total of 16. This configuration was used in States that did not have FHM before 1999. The other, which is called the C_9, is shown in figure 6B and consists of seven whole P2 cells and one-third of six other P2 cells for a total of nine. This configuration was used in States where FHM data were collected FHM before 1999. See McCollum and Cochran (2005) for details. All P2 cells have a FIA plot, and every C_{16} cell has a FHM plot, but only 5/9 of the C_9 cells contain a FHM plot. This strategy results in a FHM to FIA ratio of 1-to-16.2; note that 1/9 x 5/9 = 5/81 = 1/16.2.

(A) (B)

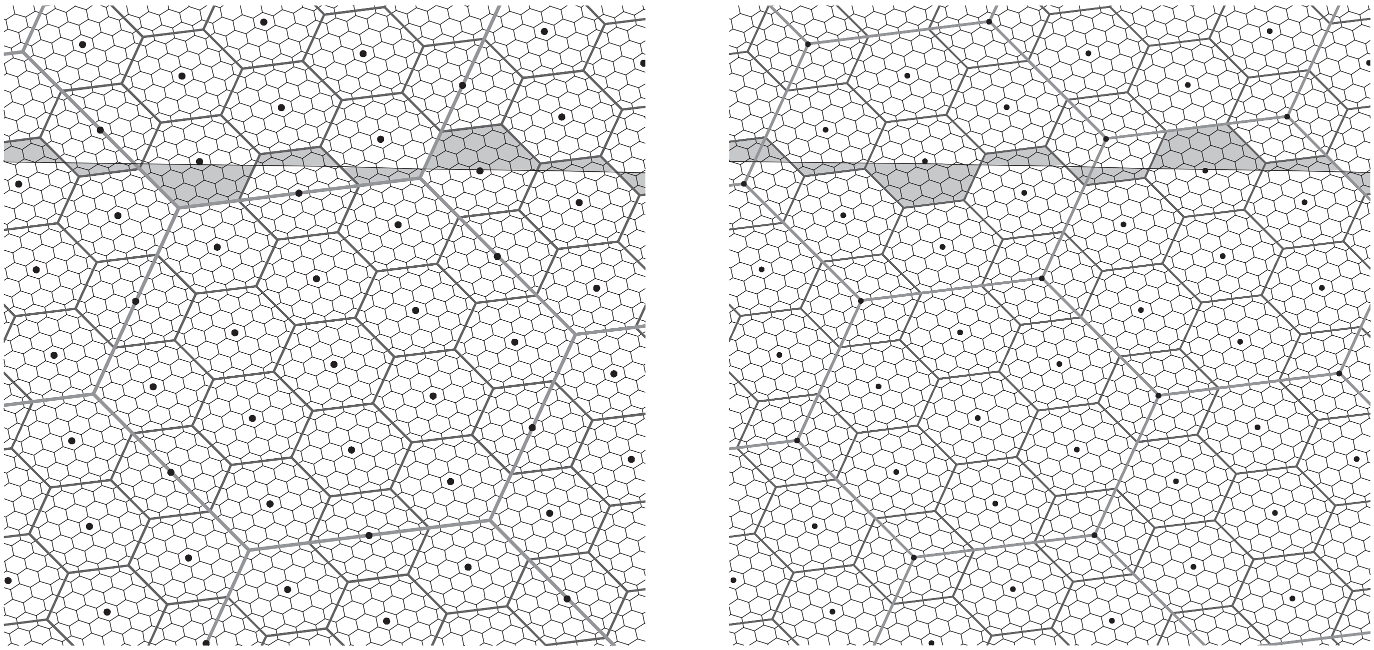

Figure 6—All three phases of FIA.

If the horizontal line in figure 6 is a State boundary, then the gray areas in figure 6 represent P1 cells that will not necessarily "belong" to corresponding P2 cells unless cells are traded between States, cells in partial hexes are ignored, or a supplemental grid assigning P1 cells to P2 cells is created. The same problem arises if remote sensing is used and pixels are used instead of dots.

If the horizontal line in figure 6 is a county boundary, other questions arise. Some analysts feel that cells in one county should not influence the data in another county. Others feel that all P2 plots should carry the same number of pixels if remote sensing is used, or the same number of photointerpretation dots if dot counting methods are used.

The authors have found a method to estimate forest area that satisfies a number of goals: the grid completely covers the landscape and maximizes the distance from one dot to the next for a fixed number of dots; placement of dots is repeatable, easily lends itself to spatial analysis, and does not require the intense investment in remote sensing, in training of analysts, or acquisition of imagery or software.

LITERATURE CITED

Brand, G.; Nelson, M.D.; Wendt, D.G.; Nimerfro, K.M. 2000. The hexagon/panel system for selecting FIA plots under an annual inventory. In: McRoberts, Ronald E.; Reams, Gregory A.; Van Deusen, Paul C., eds. Proceedings of the first annual forest inventory and analysis symposium. Gen. Tech. Rep. NC–213. St. Paul, MN: U.S. Department of Agriculture Forest Service, North Central Research Station: 8–13.

Carr, D.; Kahn, R.; Sahr, K.; Olsen, T. 1997. ISEA discrete global grids. Statistical Computing and Statistical Graphics Newsletter. 8(2/3): 31–39.

Caspar, D.; Klug, A. 1962. Physical principles in the construction of regular viruses. Cold Spring Harbor Symposium on Quantitative Biology. 27: 1–24.

Conner, R.C.; Adams, T.; Butler, B. [and others]. 2004. The state of South Carolina's forests, 2001. Resour. Bull. SRS–96. Asheville, NC: U.S. Department of Agriculture Forest Service, Southern Research Station. 67 p.

ESRI. 1991. Map projections and coordinate management. Redlands, CA: Environmental Systems Research Institute, Inc. 86 p.

Global Resource Information Database-Geneva, ed. 1992. World Databank II. Arc/Info export file. www.grida.no/db/gis/prod/html/toc.htm. [Date accessed: October 7, 2004].

McCollum, J.; Cochran, J. 2005. Forest Inventory and Analysis and Forest Health Monitoring: piecing the quilt. In: McRoberts, Ronald E.; Reams, Gregory, A.; Van Deusen, Paul C., eds. Proceedings of the fifth annual forest inventory and analysis symposium. Gen. Tech. Rep. WO–69. Washington, DC: U.S Department of Agriculture Forest Service: 182–189.

Overton, W.S.; White, D.; Stevens, D.S. 1990. Design report for EMAP environmental monitoring and assessment program. EPA/600/3-91/053. Washington, DC: U.S. Environmental Protection Agency, Environmental Monitoring and Assessment Program. 52 p.

Pearson, F., II. 1990. Map projections: theory and applications. Boca Raton, FL: CRC Press, Inc. 372 p.

Sahr, K.; White, D.; Kimerling, A.J. 2003. Geodesic discrete global grid systems. Cartography and Geographic Information Science. 30(2): 121–134.

Snyder, J.P. 1992. An equal-area map projection for polyhedral globes. Cartographica. 29(1): 10–21.

White, D.; Kimerling, A.J.; Overton, W.S. 1992. Cartographic and geometric components of a global sampling design for environmental monitoring. Cartography and Geographic Information Systems. 19(1): 5–22

McCollum, Joseph M.; Cochran, Jamie K.; Rose, Anita K. 2008. Photointerpretation on a discrete global grid. Res. Pap. SRS–44. Asheville, NC: U.S. Department of Agriculture Forest Service, Southern Research Station. 7 p.

The Forest Inventory and Analysis (FIA) Program of the Forest Service, U.S. Department of Agriculture, collects its data in three phases. The first phase is collection of photointerpretation data or dot counts, the second phase is field collection of FIA plot data, and the third phase is collection of Forest Health Monitoring data. This paper describes the development of the Phase 2 (P2) and Phase 3 (P3) grids and discusses the creation of a new grid for Phase 1 (P1), complete with an efficient indexing scheme, which is essentially equivalent to the historical dot count grids. The P2 grid consists of one field site per approximately 6,000 acres. To create the new P1 grid, we decomposed the P2 grid by a factor of 27 to obtain new proposed P1 photointerpretation cells of about 220 acres. The new grid can be used for initial photointerpretation points to determine area estimates for forested land.

Keywords: FIA, Forest Health Monitoring, global grids, hexagon, Phase 1, Phase 2, Phase 3, photointerpretation.